Biliverdin Reduction by Cyanobacterial Phycocyanobilin:Ferredoxin Oxidoreductase (PcyA) Proceeds via Linear Tetrapyrrole Radical Intermediates

ARTICLE *in* JOURNAL OF THE AMERICAN CHEMICAL SOCIETY · AUGUST 2004

Impact Factor: 12.11 · DOI: 10.1021/ja049280z · Source: PubMed

5 AUTHORS, INCLUDING:

Alexander Gunn
University of California, Davis
10 PUBLICATIONS **186** CITATIONS
SEE PROFILE

Michael D Toney
University of California, Davis
99 PUBLICATIONS **3,505** CITATIONS
SEE PROFILE

J Clark Lagarias
University of California, Davis
134 PUBLICATIONS **6,181** CITATIONS
SEE PROFILE

J|A|C|S
ARTICLES
Published on Web 06/25/2004

Biliverdin Reduction by Cyanobacterial Phycocyanobilin:Ferredoxin Oxidoreductase (PcyA) Proceeds via Linear Tetrapyrrole Radical Intermediates

Shih-Long Tu,[†] Alexander Gunn,[‡] Michael D. Toney,[‡] R. David Britt,[‡] and J. Clark Lagarias*,[†]

Contribution from the Section of Molecular and Cellular Biology and the Department of Chemistry, University of California, One Shields Avenue, Davis, California 95616

Received February 9, 2004; E-mail: jclagarias@ucdavis.edu

Abstract: Cyanobacterial phycocyanobilin:ferredoxin oxidoreductase (PcyA) catalyzes the four electron reduction of biliverdin IXα (BV) to phycocyanobilin, a key step in the biosynthesis of the linear tetrapyrrole (bilin) prosthetic groups of cyanobacterial phytochromes and the light-harvesting phycobiliproteins. Using an anaerobic assay protocol, optically detected bilin-protein intermediates, produced during the PcyA catalytic cycle, were shown to correlate well with the appearance and decay of an isotropic $g \approx 2$ EPR signal measured at low temperature. Absorption spectral simulations of biliverdin XIIIα reduction support a mechanism involving direct electron transfers from ferredoxin to protonated bilin:PcyA complexes.

Introduction

Phycocyanobilin:ferredoxin oxidoreductase (PcyA, EC 1.3.7.5) is a member of a family of ferredoxin-dependent bilin reductases (FDBRs) that includes enzymes involved in the biosynthesis of the linear tetrapyrrole prosthetic groups of the light harvesting phycobiliproteins and the photoreceptor phytochromes, as well as enzymes of the chlorophyll catabolism pathway.[1−3] Found exclusively in oxygenic photosynthetic organisms, this enzyme family can be distinguished from the NADPH-dependent biliverdin reductases BVR and BvdR [4,5] by their ferredoxin-dependency and their double bond reduction regiospecificity.[1,6] The latter property of FDBR enzymes is responsible for the large diversity of their bilin products which absorb light throughout the visible and near-IR spectral region. Based on the lack of a metal or organic cofactor, a radical mechanism was proposed for enzymes of the FDBR family, with their reduction regiospecificities reflecting enzyme-specific distribution of proton-donating side chains within the catalytic site.[7]

Unique among a family of enzymes that typically mediates two-electron reductions of their bilin substrate, PcyA catalyzes the four-electron reduction of biliverdin IXα (BV) to 3*Z*/3*E*-phycocyanobilin (PCB) as depicted in Figure 1A. We previously showed that this occurs via the two-electron reduced species 18^1,18^2-dihydrobiliverdin IXα (18^1,18^2-DHBV), indicating that the reduction of the D-ring exo-vinyl group precedes the reduction of the A-ring endo-vinyl group.[7] PcyA can also catalyze the two-electron reduction of the unnatural biliverdin XIIIα (BV13) isomer to 3*E*/3*Z*-isoPΦB (Figure 1B) as well as that of 3*Z*-phytochromobilin (PΦB) to 3*Z*-PCB (Figure 1C). Biliverdin IIIα (BV3), an unnatural isomer which possesses two exo-vinyl groups, however, is not a PcyA substrate.[7] These results indicate that exo- and endo-vinyl group reductions are not obligatorily coupled and that the vinyl substituent pattern of the BV substrate is critical for catalysis.

We previously hypothesized that the first electron is directly transferred from reduced ferredoxin to the PcyA-bound BV substrate, a process that is accompanied by (or followed by) site-specific proton transfer from a protein residue to the D-ring exo-vinyl group (Figure 1). Subsequent reduction of the monohydro-BV radical intermediate by another reduced ferredoxin molecule, together with protonation of the same exo-vinyl group by another residue in the enzyme, was envisaged to generate 18^1,18^2-DHBV. Further reduction of 18^1,18^2-DHBV to 3*Z*/3*E*-PCB presumably occurs via an analogous two step pathway, with protein residues localized near the A-ring contributing the third and fourth protons (see Figure 1). We proposed that product release is promoted by protein residues ionized during catalysis.[7] Experimental support for these hypotheses has yet to be reported.

Many enzyme systems produce organic radical intermediates during catalysis.[8] Some of these occur on protein residues, e.g., tyrosyl radicals within the photosynthetic oxygen evolution complex[9] and Class I ribonucleotide reductases,[10,11] glycyl radicals in pyruvate formate lyase[12] and tryptophanyl radicals

[†] Section of Molecular and Cellular Biology.
[‡] Department of Chemistry.

(1) Frankenberg, N.; Mukougawa, K.; Kohchi, T.; Lagarias, J. C. *Plant Cell* **2001**, *13*, 965−978.
(2) Kohchi, T.; Mukougawa, K.; Frankenberg, N.; Masuda, M.; Yokota, A.; Lagarias, J. C. *Plant Cell* **2001**, *13*, 425−436.
(3) Wuthrich, K. L.; Bovet, L.; Hunziker, P. E.; Donnison, I. S.; Hortensteiner, S. *Plant J.* **2000**, *21*, 189−198.
(4) Bell, J. E.; Maines, M. D. *Arch. Biochem. Biophys.* **1988**, *263*, 1−9.
(5) Schluchter, W. M.; Glazer, A. N. *J. Biol. Chem.* **1997**, *272*, 13562−13569.
(6) Frankenberg, N. F.; Lagarias, J. C. In *The Porphyrin Handbook. Chlorophylls and Bilins: Biosynthesis Structure and Degradation.*; Kadish, K. M., Smith, K. M., Guilard, R., Eds.; Academic Press: New York, 2003; Vol. 13, pp 211−235.
(7) Frankenberg, N.; Lagarias, J. C. *J. Biol. Chem.* **2003**, *278*, 9219−9226.
(8) Stubbe, J.; Vanderdonk, W. A. *Chem. Rev.* **1998**, *98*, 705−762.

10.1021/ja049280z CCC: $27.50

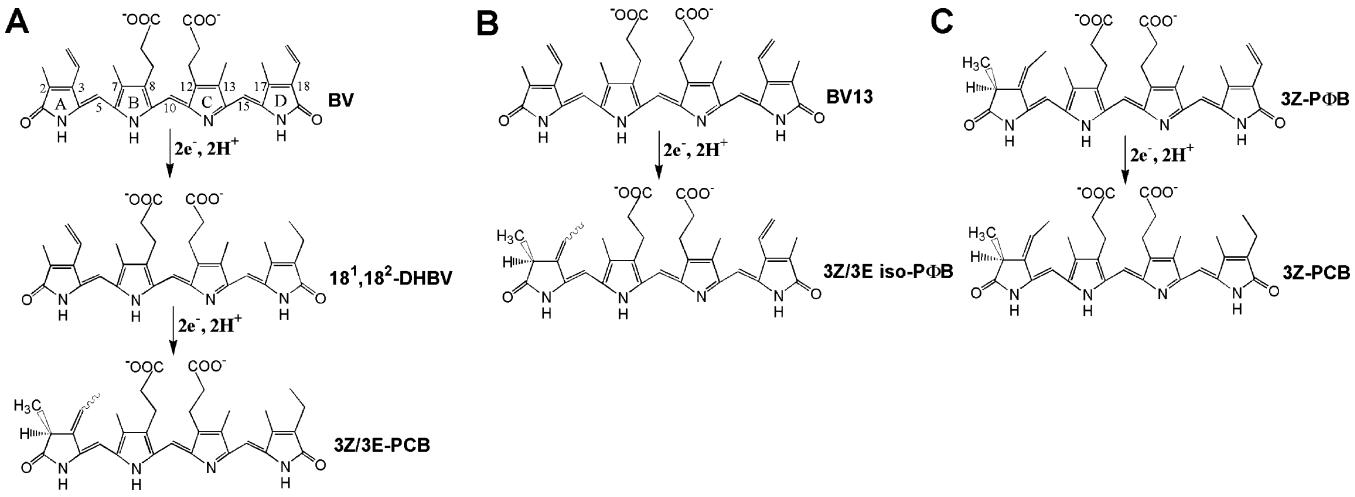

Figure 1. Bilin substrates, intermediates, and products of phycocyanobilin:ferredoxin oxidoreductase (PcyA). PcyA mediates the four-electron reduction of biliverdin IXα (BV) to 3*Z*/3*E*-phycocyanobilin (PCB) (panel A) via the intermediacy of the two-electron reduced stable intermediate $18^1,18^2$-dihydrobiliverdin IXα ($18^1,18^2$-DHBV). PcyA also mediates two-electron reductions of biliverdin XIIIα (BV13) to 3*Z*/3*E*-isophytochromobilin (3*Z*/3*E*-isoPΦB) (panel B) and of 3*Z*-PΦB to 3*Z*-PCB (panel C).

in cytochrome *c* peroxidase.[13] Other radical enzymes possess tightly bound organic and/or metal ion cofactors that catalyze single-electron transfers, e.g., monoamine oxidase,[14] ferredoxin-dependent pyruvate reductase,[15] benzoyl-CoA reductase,[16] and Class II/III ribonucleotide reductases.[17] Because of the lack of an organic or metal ion cofactor that mediates one-electron transfers from reductant to substrate, FDBRs represent a new class of radical enzymes.

The present work was undertaken to address the hypothesis that PcyA-mediated bilin reduction proceeds via tetrapyrrole radical intermediates. Using an anaerobic assay protocol that eliminated oxidation of organic radicals and/or ferredoxin, we report the optical detection of novel species produced during sequential electron transfers to preformed PcyA:BV complexes. Direct evidence for organic radical intermediates using electron paramagnetic resonance (EPR) spectroscopy at low temperature was correlated with the appearance and decay of these novel protein-bound bilin species. To simplify the number of bilin species produced, experiments were also performed using the two-electron substrate BV13. Such analyses facilitated resolution of the spectroscopic properties of the PcyA complexes with its bilin substrate, semireduced intermediate(s), and isoPΦB product. These studies not only provided evidence for the formation of bilin radical intermediates during catalysis but also permitted development of mechanistic models for bilin reduction by this interesting oxidoreductase family.

Results

Anaerobic Assay Development. Previous studies on PcyA were performed using substrate excess (i.e., turnover conditions) with no precautions to remove oxygen.[7] To detect radical intermediates, we developed new assay conditions to both limit the number of electron-transfer reactions and avoid oxidation of ferredoxin and/or potential radical intermediates. The reaction temperature was decreased to 16 °C to slow the reaction, and NADPH was used instead of an NADPH regenerating system to permit addition of defined amounts of reductant into reaction mixtures. In our experimental setup, PcyA:BV complexes were prepared prior to addition of reductant. Reduction of PcyA:BV therefore requires that oxidized ferredoxin (Fd_{ox}) must first be reduced via NADPH and ferredoxin:$NADP^+$ oxidoreductase (FNR). The rapid rate of FNR-mediated reduction of Fd_{ox} expected under our experimental conditions[18,19] and the absence of stable complex formation between Fd and PcyA (unpublished data) suggested that the rate of PcyA:BV reduction could be controlled by FNR concentration. By using small amounts of FNR in the assay system, BV reduction could be controlled to permit kinetic spectroscopic measurements in the second to minute time scale. The nanomolar concentration of FNR in these assay mixtures also minimized the potential formation of flavin radical species which could be mistaken for tetrapyrrole radical intermediates. Using the standard assay conditions described under Experimental Procedures, catalysis could be monitored using a conventional absorption spectrophotometer, and aliquots could easily be removed for analysis by HPLC and low-temperature EPR spectroscopy.

Absorption Spectral Evidence for Semireduced Intermediates. Standard bilin reductase assays under anaerobic conditions used 10 μM preformed PcyA:BV complexes in quartz cuvettes to which sequential additions of 1 electron equiv of NADPH (i.e., 5 μM NADPH) were added with stirring. Significant spectral changes were observed following the addition of the first equivalent of NADPH (Figure 2A, 1 equiv e^-). Rapid absorption changes occurred throughout the visible spectral region upon NADPH addition, with notable increases occurring at 470 and 770 nm. These absorbance increases

(9) Gilchrist, M. L. J.; Ball, J. A.; Randall, D. W.; Britt, R. D. *Proc. Natl. Acad. Sci. U.S.A.* **1995**, *92*, 9545−9549.
(10) Sjoberg, B. M.; Reichard, P. *J. Biol. Chem.* **1977**, *252*, 536−541.
(11) Stubbe, J.; Nocera, D. G.; Yee, C. S.; Chang, M. C. Y. *Chem. Rev.* **2003**, *103*, 2167−2201.
(12) Wagner, A. F.; Frey, M.; Neugebauer, F. A.; Schafer, W.; Knappe, J. *Proc. Natl. Acad. Sci. U.S.A.* **1992**, *89*, 996−1000.
(13) Sivaraja, M.; Goodin, D. B.; Smith, M.; Hoffman, B. M. *Science* **1989**, *245*, 738−740.
(14) Silverman, R. B. *Acc. Chem. Res.* **1995**, *28*, 335−342.
(15) Menon, S.; Ragsdale, S. W. *Biochemistry* **1997**, *36*, 8484−8494.
(16) Boll, M.; Fuchs, G.; Lowe, D. J. *Biochemistry* **2001**, *40*, 7612−7620.
(17) Eklund, H.; Uhlin, U.; Farnegardh, M.; Logan, D. T.; Nordlund, P. *Prog. Biophys. Mol. Biol.* **2001**, *77*, 177−268.
(18) Martinez-Julvez, M.; Hermoso, J.; Hurley, J. K.; Mayoral, T.; Sanz-Aparicio, J.; Tollin, G.; Gomez-Moreno, C.; Medina, M. *Biochemistry* **1998**, *37*, 17680−17691.
(19) Medina, M.; Martinez-Julvez, M.; Hurley, J. K.; Tollin, G.; Gomez-Moreno, C. *Biochemistry* **1998**, *37*, 2715−2728.

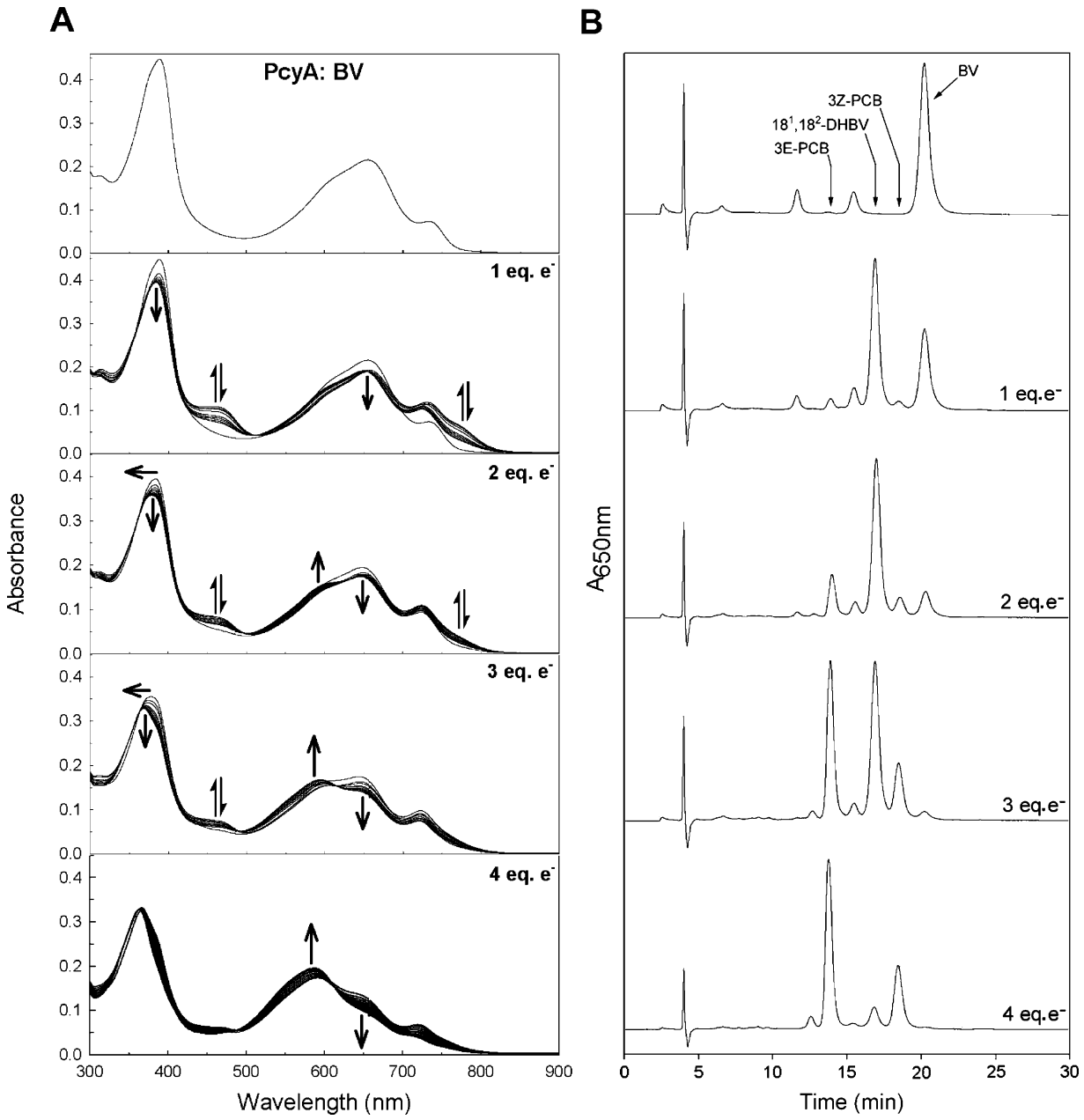

Figure 2. Absorption spectra and HPLC analysis of PcyA-catalyzed biliverdin IXα reduction under anaerobic conditions. The time course of BV reduction by PcyA was monitored spectrophotometrically (panel A) and by HPLC (panel B) following sequential addition of 1 to 4 molar equiv of reductant (i.e., 5 μM NADPH) to samples containing 10 μM PcyA:BV complex, 3 nM FNR, 10 μM Fd and an oxygen scavenging system as described under Experimental Procedures. Absorption spectra were monitored for 10 min; 1 min intervals are shown. Periods of 20 min were provided between subsequent additions of NADPH. Absorbance increases followed by decays at 470 and 770 nm were indicated by double arrows, while absorbance decreases at 380 and 650 nm and increases at 590 nm were indicated by single arrows. Reaction mixture aliquots (200 μL) corresponding to the spectra shown in panel A were withdrawn, and extracted bilin pigments were analyzed by reversed-phase HPLC as described in Experimental Procedures (panel B). Elution positions of BV, 3Z-PCB, 3E-PCB, and 18^1,18^2-DHBV standard are indicated by arrows, and absorbance at 650 nm was monitored.

occurred within the first 2 min after NADPH addition and were followed by a slower decay over the next 10−20 min (Figure 2A). A smaller absorption decrease at 650 nm occurred concomitantly with these rapid increases that was not followed by further changes. The absorbance increase at 470 nm indicated the production of a new species of "rubin-like" pigment during catalysis, possibly corresponding to a semireduced radical intermediate. Absorbance increases and decays at 470 and 770 nm were observed with nearly identical kinetics, indicating that these changes reflect a single semireduced species or a mixture of kinetically indistinguishable species which decay by the same rate-limiting step. Sequential addition of 2 to 4 electron equiv produced similar rapid absorbance increases that also were followed by slow decays (Figure 2A). The pronounced blue shift at 380 nm and absorbance increase at 590 nm in the spectra recorded after addition of the second and third equivalent of NADPH addition reflected the formation of reaction products, 3*Z*- and 3*E*-PCB. In this regard, a very similar spectrum was produced upon mixing equimolar concentrations of 3*E*-PCB with PcyA (data not shown).

HPLC Analyses of Product Distribution. In parallel with the above experiments, product analysis was performed by HPLC following addition of 1 electron equiv (i.e., 50 mol % NADPH) and removal of sample aliquots after absorbance

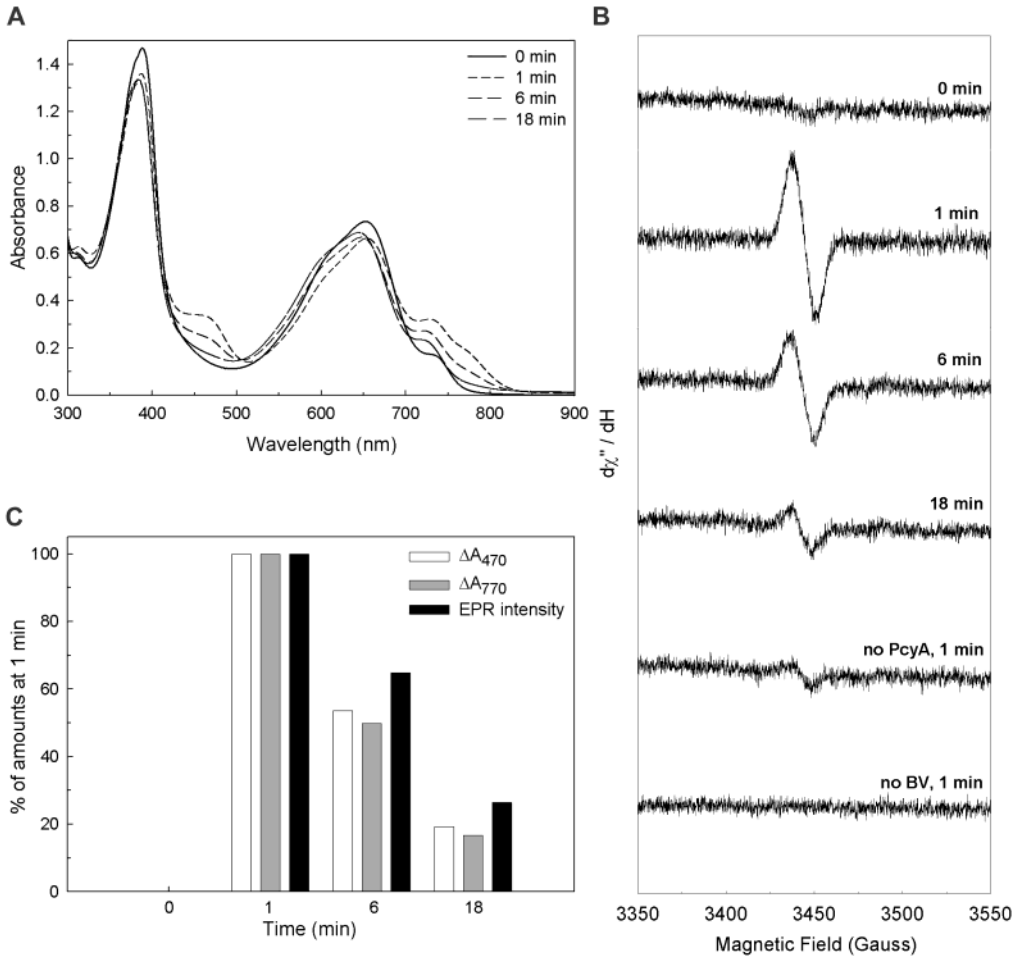

Figure 3. BV reduction time courses monitored by absorption and low-temperature EPR detection of an exo-vinyl bilin radical. The time course of BV reduction by PcyA was monitored by spectrophotometry (panel A) and by low-temperature EPR spectroscopy (panel B) following addition of 1 molar equiv of reductant (i.e., 20 μM NADPH) to samples containing 40 μM preformed PcyA:BV complexes as described under Experimental Procedures. Absorption spectra were taken at time 0 min (—), 1 min (- - -), 6 min (— — —), and 18 min (— —) after NADPH addition. For EPR measurement, 200 μL aliquots were withdrawn at the times indicated and were immediately frozen in liquid nitrogen. EPR spectra at 15 K were recorded at 9.69 GHz. Control samples lacking PcyA enzyme or BV substrate are shown. Panel C shows the relative EPR signal intensity and relative absorbance at 470 and 770 nm normalized to the % of the signal at 1 min.

changes were complete (Figure 2B). This analysis shows that only 18^1,18^2-DHBV and unreacted BV substrate were present in roughly equimolar proportions after addition of 1 electron equiv. Since 18^1,18^2-DHBV is the two-electron reduced stable intermediate,[7] its production indicates that two-electron transfers had occurred from two separate reduced ferredoxin molecules and/or that some semireduced intermediates had disproportionated. The rapid appearance and slow decay of the spectral intermediates described above suggest that the latter had occurred, but it was not possible to rule out two sequential electron transfers. The roughly 50:50 mixture of 18^1,18^2-DHBV and BV after 1 electron equiv supports the hypothesis that the transient spectral signatures observed arose from semireduced, unstable intermediates that subsequently decay into 18^1,18^2-DHBV and BV. HPLC analyses were also performed following addition of the second, third, and fourth electron equivalents (Figure 2B). Following addition of a second electron equivalent, nearly all of the BV substrate was converted to 18^1,18^2-DHBV and some 3Z/3E-PCB, the four-electron reduced final product. Subsequent addition of third and fourth electron equivalents led to complete conversion of remaining 18^1,18^2-DHBV to 3*Z*/3*E*-PCB product. Taken together, these measurements establish that all of the BV substrate is converted to 3*Z*/3*E*-PCB product and that the spectrally observed transient species correspond to semireduced, unstable intermediates produced upon electron transfers to PcyA:BV and PcyA:18^1,18^2-DHBV complexes.

EPR Detection of the Exo-Vinyl Bilin Radical Intermediate. To detect a radical intermediate, we performed EPR measurements on freeze-quenched PcyA:BV samples following addition of reductant. To improve the signal-to-noise ratio, PcyA:BV and FNR concentrations were increased 4-fold, to 40 μM and 12 nM, respectively (see Experimental Procedures). Spectroanalytical-grade glycerol also was added to the reaction mixtures for cryoprotection and minimization of intermolecular interactions. The UV−vis spectrum of the reaction mixture was analyzed after addition of 1 equiv of NADPH and showed the characteristic absorbance changes seen for less concentrated mixtures (Figure 3A). Aliquots were removed at time 0, 1, 6, and 18 min, frozen in liquid nitrogen, and analyzed by EPR spectroscopy at 15 K (Figure 3B). These measurements revealed isotropic EPR signals at $g \approx 2$ with a peak to trough width of 15 G which rapidly appeared and slowly decayed following NADPH addition. The time-dependent changes in relative absorbance at 470 nm and EPR signal strengths, both normalized to their maximum values 1 min after addition of NADPH, are illustrated in Figure 3C. These data show that the EPR-detectable

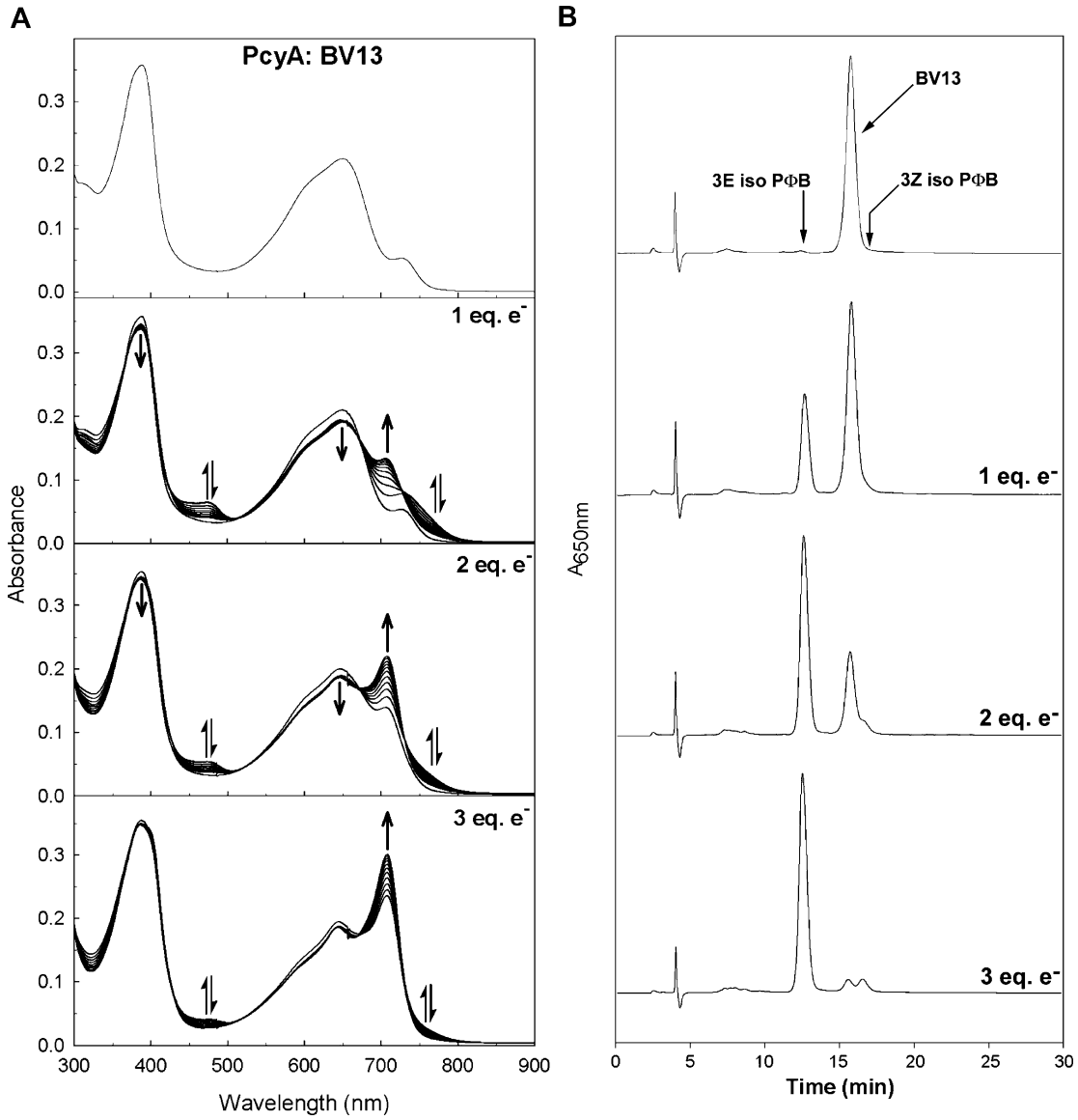

Figure 4. Absorption spectra and HPLC analysis of PcyA-catalyzed biliverdin XIIIα (BV13) reduction under anaerobic conditions. The time course of BV13 reduction by PcyA was monitored by spectrophotometry (panel A) and by HPLC (panel B) following sequential addition of 1 to 3 molar equiv of reductant was performed identically to that shown in Figure 2. Absorbance increases and decays at 474 and 760 nm were indicated by double arrows, while absorbance decreases at 380 and 650 nm and increases at 710 nm were indicated by single arrows. Reaction mixture aliquots (200 μL) corresponding to the spectra shown in panel A were withdrawn and analyzed as described in Figure 2. Elution positions of BV13, 3*Z*-isoPΦB, and 3*E*-isoPΦB standards are indicated by arrows.

intermediate appeared and decayed with the same kinetics as that responsible for the absorbance changes. Control measurements on samples lacking either PcyA or BV indicated that the EPR signals corresponded to a semireduced PcyA:bilin complex rather than components of the assay mixture. A small signal was observed in the control experiment lacking PcyA, suggesting that chemical reduction of BV by ferredoxin may occur under these conditions. In this case, however, no bilin products attributed to 18^1,18^2-DHBV, PΦB, or PCB could be detected by HPLC (data not shown). When taken together, these measurements strongly support the production of bilin radical species during PcyA-mediated exo-vinyl reduction of BV.

Detection of the Endo-Vinyl Bilin Radical Intermediate. PcyA possesses two separate catalytic activities, i.e., 18^1,18^2-DHBV:ferredoxin oxidoreductase and PCB:ferredoxin oxidoreductase activities.[7] The 18^1,18^2-DHBV:ferredoxin oxidoreductase activity mediates the two-electron reduction of the D-ring exo-vinyl group of BV, while the PCB:ferredoxin oxidoreductase activity mediates the two-electron reduction of the A-ring endo-vinyl group of 18^1,18^2-DHBV. The above experiments have confirmed the production of a radical intermediate during exo-vinyl reduction of BV. Because of the reduced complexity of a two electron substrate, BV13 was used to examine whether PcyA-mediated endo-vinyl group reduction also proceeds via a radical intermediate(s). We previously showed that BV13 is converted to 3*Z*/3*E*-isoPΦB by PcyA (Figure 1B), indicating that PcyA catalyzes only A-ring reduction of this substrate.[7] Using the identical assay protocol as described for BV substrate, the course of PcyA-mediated reduction of BV13 was monitored by absorption, HPLC, and EPR spectroscopy.

Figure 4A shows the absorption changes that accompany the reduction of BV13 by PcyA. Similar to BV experiments, addition of a 1 electron equiv to the preformed PcyA:BV13

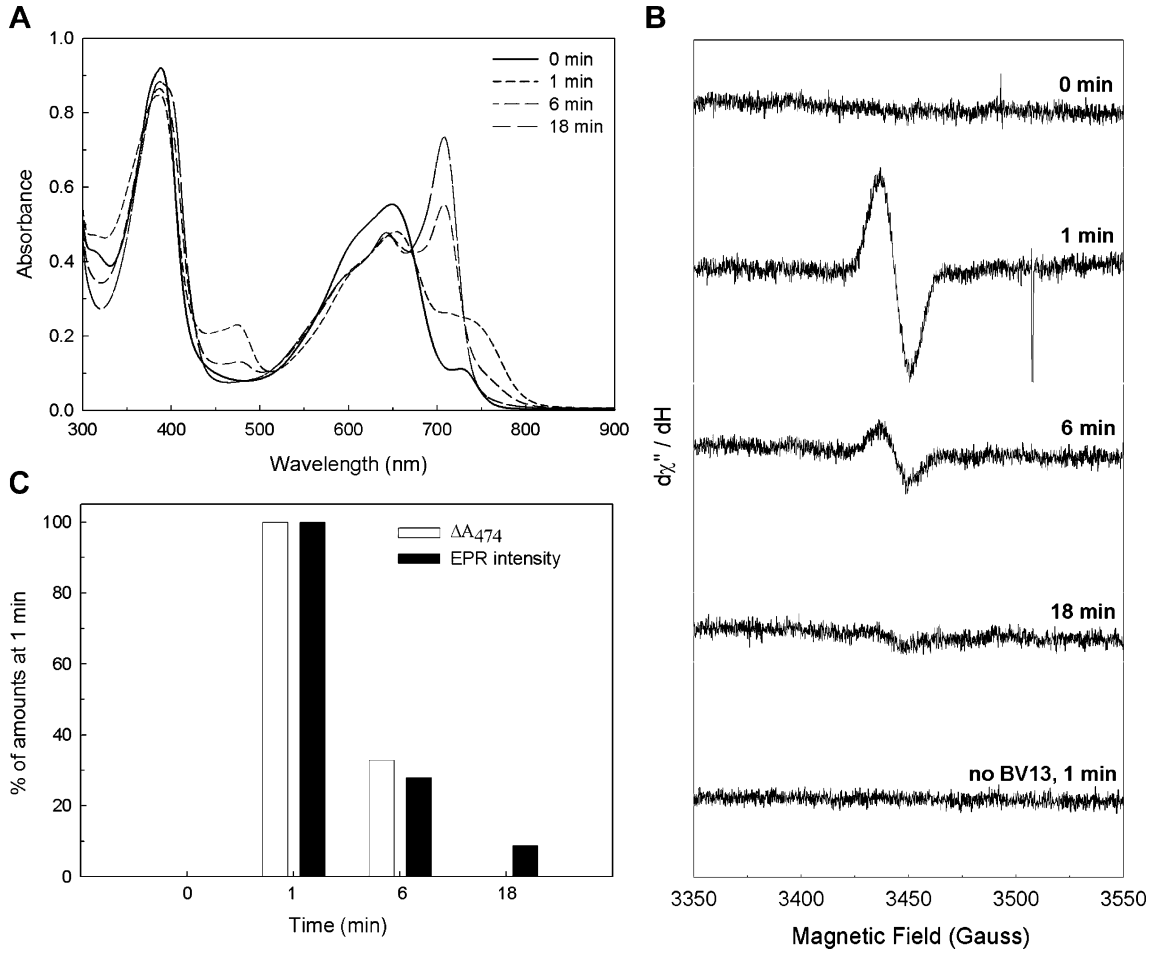

Figure 5. BV13 reduction time courses monitored by absorption and low-temperature EPR detection of the endo-vinyl bilin radical. The time course of BV13 reduction by PcyA was monitored by spectrophotometry (panel A) and by low temperature EPR spectroscopy (panel B) following addition of 1 molar equiv of reductant that was performed identically to that described in Figure 3. Absorption spectra and low-temperature EPR spectra on samples removed at time 0 min (—) and 1 min (- - -), 6 min (— — —), and 18 min (— —) after NADPH addition are shown. Panel C shows the relative EPR signal intensity and relative absorbance at 474 nm normalized to the % of the signal at 1 min.

complex led to rapid absorbance increases at 474 and 760 nm that were followed by a slower decay. Addition of the second electron equivalent produced similar spectral changes to those observed for BV, with the exception that a prominent absorbance at 710 nm appeared. A third equivalent was needed to fully convert BV13 substrate to product. HPLC analysis confirmed that the absorption changes correlated with the two-electron conversion of BV13 to isoPΦB (Figure 4B). In contrast with BV experiments, only the 3*E*-isomer of isoPΦB was produced. In this regard, reconstitution of PcyA with 3*E*-isoPΦB yielded a complex with the identical absorption spectrum as the final PcyA:bilin product (data not shown). The transient appearance and decay of new spectroscopically detectable species were very similar to those observed with BV substrate, suggesting that radical species were produced upon reduction of BV13. To test this hypothesis, low-temperature EPR spectroscopy was performed on anaerobic PcyA:BV13 preparations to which 1 electron equiv of NADPH was added. As showed in Figure 5, the appearance of a $g \approx 2$ EPR signal was well correlated with the production and decay of the absorbance changes at 474 nm. When taken together, these results indicate that the PcyA-mediated BV13 reduction also proceeds via an endo-vinyl radical intermediate, thereby implicating two bilin radical intermediates in the four-electron reduction of BV by PcyA.

Spectral Analysis of PcyA:BV13 Reduction. The spectra for the PcyA:BV13 "substrate", the semireduced PcyA:BV13 "intermediate", and the PcyA:3*E*-isoPΦB "product" (Figure 6) were each obtained from global analysis of the kinetic absorption changes using the program SpecFit32 and the kinetic scheme described in Experimental Procedures. Since absorption spectra of linear tetrapyrroles reflect mixtures of many possible conformers, tautomers, and/or (de)protonated species,[20] the measured spectra were resolved into log-normal distribution curves, a method that has proven useful to determine cofactor tautomer compositions in pyridoxal phosphate-dependent enzymes.[21] The most parsimonious choice of log-normal distribution curves that described the absorption spectra of the three PcyA:bilin complexes are shown in Figure 6. The sum of the calculated log-normal distribution curves for each species, depicted as dashed lines, fitted the experimentally determined spectra with correlation coefficients of 0.999.

To assign the log-normal spectral distribution curves to actual chemical species, AM1 and ZINDO calculations were performed using a BV13 "model" compound with two endo vinyl groups and methyl groups replacing the propionate side chains. Various

(20) Falk, H. *The Chemistry of Linear Oligopyrroles and Bile Pigments*; Springer-Verlag: Vienna, 1989.
(21) Metzler, C. E.; Metzler, D. E. *Anal. Biochem.* **1987**, *166*, 313−327.

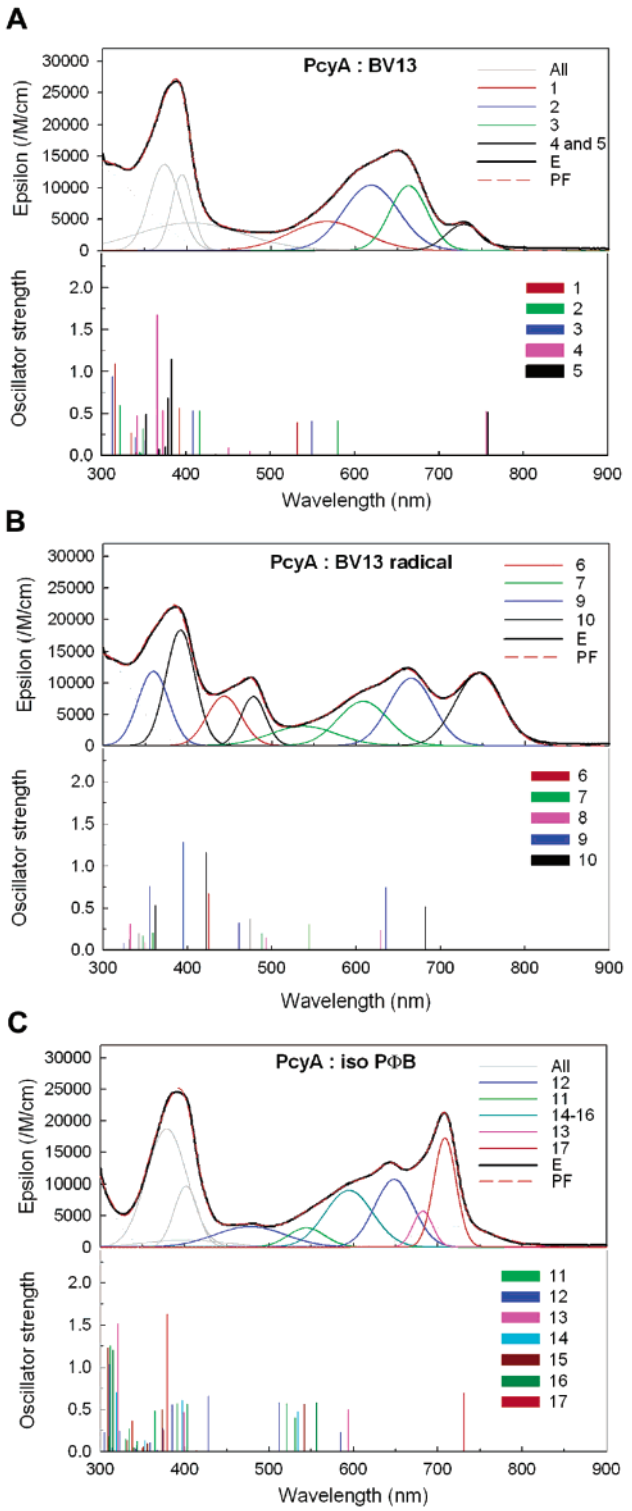

Figure 6. Simulated absorption spectra of the PcyA complex with BV13 substrate, the semireduced intermediate mixture, and isoPΦB product. Experimentally determined absorption spectra of PcyA:BV13 substrate (panel A), PcyA:intermediate (panel B), and the PcyA:isoPΦB product (panel C) are shown. Log-normal distribution curve fits shown as smooth colored curves were determined using PeakFit as described under Experimental Procedures. The sum of the log-normal distribution curves for each spectrum is shown as dashed lines labeled PF that is superimposed on each experimentally determined spectrum labeled E. ZINDO-calculated absorption maxima and oscillator strengths of AM1-optimized model compounds labeled 1−17 are shown in the bottom half of panels A−C (see Table 1 for model compound structures). Assignments of the calculated spectra with the log-normal distribution curves are shown in the same color. See text for details.

Table 1. Neutral and Protonated Biliverdin XIIIα (BV13), Semireduced BV13-derived Intermediates, and Isophytochromobilin (isoPΦB) Product Model Compounds Used for AM1 and ZINDO Calculations[a]

tautomers	PcyA/BV13	charge
1	BV13 lactam N124H	neutral
2	BV13 lactim N34H O1H	neutral
3	BV13 lactim N24H O1H	neutral
4	BV13H lactim N234H O1H	cation
5	BV13H lactam N1234H	cation
tautomers	PcyA:BV13 radical	charge
6	BV13H lactam 1e	neutral
7	MHBV13H lactam 1e (C2H)	cation
8	MHBV13H lactim 1e (O1H)	cation
9	MHBV13H lactam 2e (C2H)	neutral
10	MHBV13H lactim 2e (O1H)	neutral
tautomers	PcyA:isoPΦB	charge
11	3*E*-isoPΦB lactam N124H	neutral
12	3*E*-isoPΦB lactam N134H	neutral
13	3*E*-isoPΦB lactim N24H O1H	neutral
14	3*E*-isoPΦB lactim N34H O1H	neutral
15	3*E*-isoPΦB lactim N12H O19H	neutral
16	3*E*-isoPΦB lactim N13H O19H	neutral
17	3*E*-isoPΦB lactam N1234H	cation

[a] The structures of the AM1 optimized model compounds numbered 1−17 in this table are included in Supporting Information. AM1 and ZINDO calculations were performed using the Gaussian 98 suite of programs as described in Experimental Procedures.

tautomers of this model compound were energy minimized, with the experimental constraint to cyclic, porphyrin-like conformations based on the measured absorption spectra of PcyA:bilin complexes described previously.[7] Since the number of potential bilin species is large, we confine our discussion to the bilins shown in Table 1, which will be incorporated into a mechanistic model presented in Figure 7. After geometry optimization of lactam and lactim tautomers of BV13 substrate, potential one- and two-electron reduced "intermediates" and 3*E*-isoPΦB product using AM1, ZINDO calculations were performed to determined the electronic transitions of each tetrapyrrole structure (i.e., wavelength maxima and oscillator strengths). The results of these calculations are shown in Figure 6 (lower panels).

For neutral PcyA:BV13 "substrate" model compounds, the calculated absorption spectra typically consisted of two classes of absorption transitions, one clustering in the visible between 550 and 700 nm and a second in the near UV between 300 and 400 nm (Figure 6A). Protonated "cationic" or deprotonated "anionic" BV13 species were the only species examined which exhibited electronic transitions greater than 700 nm. Only protonated BV13 model compounds are shown in Figure 6A, since a bilin anion substrate is unlikely to be the primary electron acceptor. Based on these analyses, the spectrum of the PcyA:BV13 complex best corresponds to the electronic transitions of a mixture comprised of neutral lactam and lactim tautomers with λ_{max} at 565, 618, and 662 nm and protonated cationic BV13 with a λ_{max} at 728 nm. We previously showed that the long wavelength absorption maximum was observed only for bilin:PcyA complexes which could undergo catalysis, suggesting that the chemical species responsible for this spectral signature is the direct electron acceptor.[7] A protonated BV structure was therefore assigned to this long wavelength absorption maximum.

The spectrum of the semireduced PcyA:BV13 intermediate was considerably more complex than that of PcyA:BV13 (Figure 6B), exhibiting a pronounced new absorption maximum in the blue (i.e., λ_{max} at 443 and 477 nm), in the green to red region

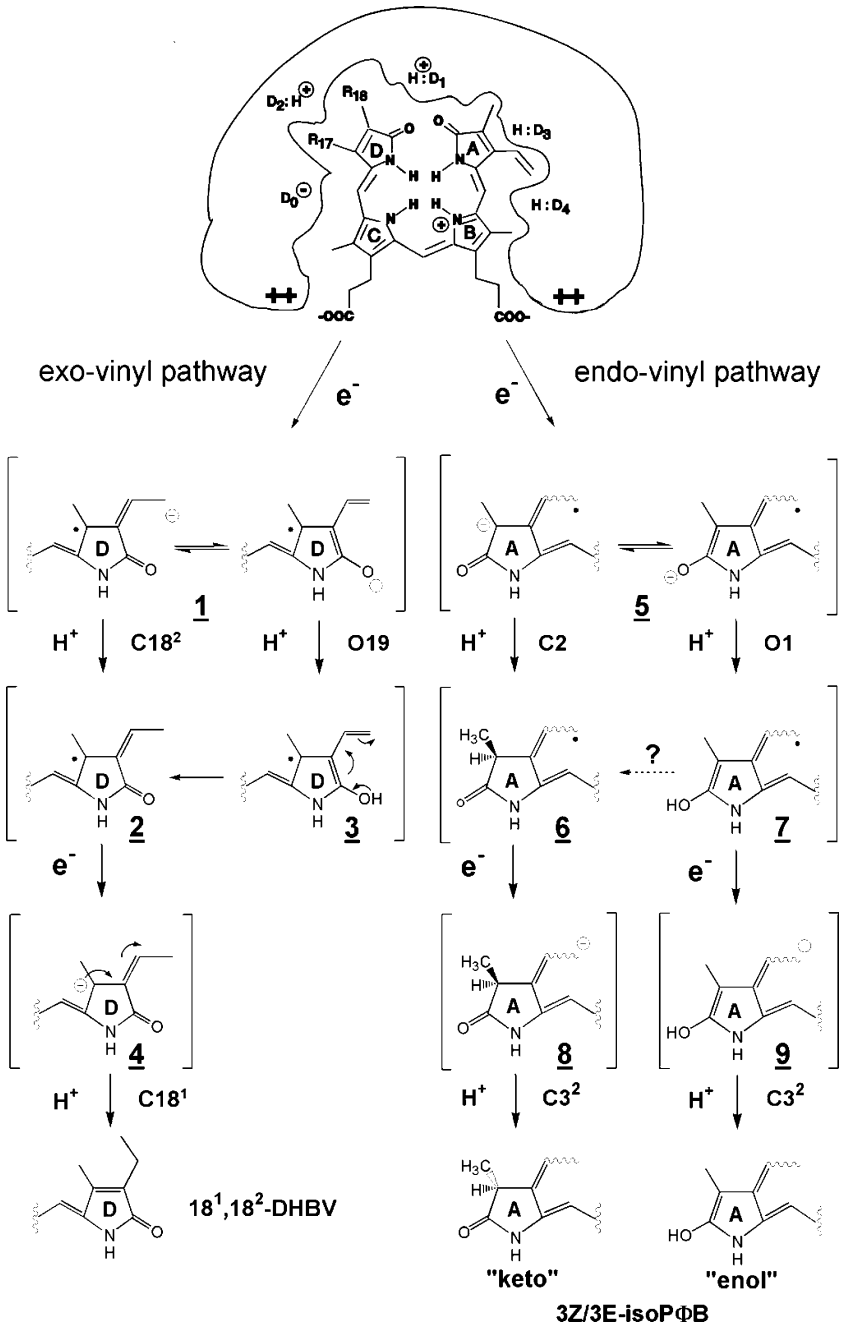

Figure 7. Proposed mechanisms for PcyA-catalyzed exo-vinyl and endo-vinyl group reductions. Substrates BV and BV13 bind to PcyA in a cyclic, porphyrin-like conformation. Protonation of the bilin substrate by proton-donating residue D_0 facilitates electron transfer from reduced ferredoxin. For the exo-vinyl pathway, the one-electron reduced neutral BV radical **1** (shown in two resonance structures) becomes protonated by residue D_1 on either carbon atom $C18^2$ or oxygen atom O19 to generate the cation radicals **2** or **3**. Through intramolecular tautomerization, species **3** should readily convert to species **2**. The second electron transfer produces the most long-lived intermediate **4**, which upon protonation on the $C18^1$ position by residue D_2 yields $18^1,18^2$-DHBV. For the endo-vinyl pathway, the one-electron reduced neutral BV13 radical **5a** (R_{18} = methyl and R_{17} = vinyl) or the neutral $18^1,18^2$-DHBV radical **5b** (R_{18} = vinyl and R_{17} = methyl) becomes protonated by residue D_3 on either carbon atom C2 or oxygen atom O1 to generate the cation radicals **6** and/or **7**. The second electron transfer produces the long-lived intermediate **8** and/or **9**, which upon protonation on the $C3^2$ position by residue D_4 yields "keto" and "enol" forms of 3*Z*/3*E*-isoPΦB or 3*Z*/3*E*-PCB products.

(i.e., λ_{max} at 537 nm, 608, and 664 nm), and in the near-infrared (i.e., λ_{max} at 745 nm). ZINDO calculations were performed on a large number of potential one-electron reduced bilins, i.e., BV13 radical anions, neutral BV13 radicals, and cationic MHBV13 radicals; however, only the latter two species yielded spectra with visible electronic transitions. The blue absorption maxima are consistent with the one-electron reduced lactam neutral radical as well as the neutral two-electron reduced species that had been protonated on either C18- or O19-positions. Absorption maxima at 537, 608, and 664 nm correspond well with the calculated electronic transitions of the one-electron reduced "cationic" monohydrobiliverdin (MHBV) species that also had been protonated on either C18- or O19-positions. Based on our calculations, the absorption maximum at 745 nm can best be attributed to a two-electron reduced "neutral" MHBV13 intermediate. The presence of this species is reasonable assuming (1) that the rate of the second electron transfer to the cationic MHBV13 radical intermediate complex

is similar to that of the first electron transfer to PcyA:BV13 and (2) that the penultimate protonation of the two-electron reduced "neutral" MHBV13 intermediate complex is rate-limiting. With these assumptions, the appearance and decay of both one-electron and two-electron reduced species would be kinetically indistinguishable. The complexity of the absorption spectrum of the semireduced "intermediate" therefore reflects the mixture of one- and two-electron reduced BV13 species.

Similar to the PcyA:BV13 substrate complex, the spectrum of the PcyA:isoPΦB product complex consisted of two classes of absorption transitions which we assign to neutral lactam and lactim tautomers (Figure 6C). The pronounced maximum at 708 nm of this complex is in good agreement with the calculated spectrum of the cationic isoPΦB lactam. This transition is considerably more enhanced than that attributed to the protonated BV13 lactam substrate complex indicating that the pK_a and/or environment of isoPΦB is distinct from those of the BV13 substrate. By comparison with the PcyA:isoPΦB product complex, the spectrum of the four-electron reduced PcyA:PCB product complex (see Figure 2A, bottom panel, 4 equiv e−) showed little enhancement of this infrared absorption maximum. This difference may reflect the fact that BV13 possesses two endo-vinyl groups and no exo-vinyl group. In this regard, proton-donating residues which contribute to the initial exo-vinyl reduction of BV are still present in their protonated forms in the PcyA:isoPΦB product complex and thereby could influence the latter's spectrum. The presence of a second endo-vinyl group in the PcyA:isoPΦB product complex might also account for this enhancement.

Discussion

PcyA Mediates Sequential One-Electron Transfers from Ferredoxin to the Enzyme-Bound Bilin Substrate(s). Using an anaerobic coupled electron-transfer assay system, the present studies provide direct spectroscopic support for the production of bilin radical intermediates during PcyA-mediated BV reduction. Our studies show that NADPH-dependent absorption changes correlate well with the appearance/decay of EPR-detectable organic radical intermediates and with the appearance of stoichiometric amounts of the 18^1,18^2-DHBV intermediate and/or PCB product. These investigations clearly establish that PcyA-mediated reduction of BV to PCB proceeds via four one-electron transfers from individual reduced ferredoxin molecules to tightly associated PcyA:bilin complexes.

The present experiments indicate that the EPR-detectable bilin radical intermediates are quite stable, decaying with a half-life between 10 and 20 min. We believe that this slow rate of decay is due to disproportionation of the PcyA:bilin radical intermediate(s), a process that generates stoichiometric amounts of oxidized starting material and two-electron reduced intermediate/product. In this regard, studies on the electron-transfer flavoprotein (ETF):ubiquinone (Q) oxidoreductase have showed that ETF reduction can occur via disproportionation of two flavin radicals.[22] PcyA is a monomer, however, and there is no evidence for the formation of dimers.[7] In view of the slow rate of radical decay, we envisage that random "productive" collisions between two PcyA:bilin radical complexes are responsible for this protein-to-protein electron transfer. The disproportionation proposal is further supported by the analyses of product stoichiometry using HPLC and by the concentration-dependence of the radical decay (Tu, S.-L.; Lagarias, J. C. Unpublished data). These results show that initial one-electron transfer to the PcyA:bilin complex is reversible, providing additional evidence in support of a sequential one-electron-transfer mechanism.

Bilin radicals have been proposed as intermediates in the photochemical oxidation and thiol addition reactions of rubins[20,23,24] and also have been implicated in various nonphotochemical interconversions of bilins.[25,26] The enzyme-mediated intermediacy of bilin radicals however has no literature precedent to our knowledge. The production of such radicals in oxygenic photosynthetic organisms requires a mechanism to sequester these radicals from molecular oxygen. In this regard, FDBR family members PcyA and HY2 efficiently catalyze the aerobic reductions of BV to PCB[7] and to PΦB,[27] respectively, suggesting that bilin radical intermediates must be buried inside both enzymes or otherwise made inaccessible to direct reaction with molecular oxygen. BV reduction is, however, much more efficient under anaerobic conditions used here than that described previously,[7] as the PCB product yield is greatly improved from assays performed aerobically (data not shown). Side reactions of bilin radical intermediates with molecular oxygen and/or reactions between the bilin substrates/products with ferredoxin-generated reduced oxygen species (i.e., O_2^- and H_2O_2) are probably responsible. In this regard, BV is quite sensitive to chemical reactions with superoxide and/or peroxide.[20,23,24] These side reactions are expected to be mitigated by the presence of powerful molecular oxygen and oxidant scavenging systems found in cyanobacterial cells; however, it remains an interesting dilemma with which oxygenic photosynthetic organisms that contain these enzymes must cope.

Mechanistic Implications. Spectroscopic measurements described in this work provide new insight into the mechanism of bilin reduction by PcyA. Since PcyA catalyzes two distinct vinyl group reductions, our proposed mechanism shown in Figure 7 addresses both exo- and endo-vinyl group reduction reactions. In neutral to basic aqueous solution, free BV adopts a porphyrin-like lactam conformation.[20] Based on the absorbance spectra of PcyA:bilin complexes, the bilin substrate also appears to adopt a cyclic conformation with A and D rings buried within the enzyme and the propionate side chains extended toward the solvent.[7] In this regard, the absorption spectra of PcyA:bilin substrates are very similar to those of BV complexes with myoglobin[28,29] and heme oxygenase,[30] both of which constrain BV to cyclic conformations. Unlike the latter two complexes, all PcyA:bilin substrate complexes possess near-infrared absorption maxima, a spectral feature that is correlated with their ability to be reduced.[7] Based on ZINDO calculations, we have assigned this spectral signature to an N-protonated, cyclic BV structure

(22) Ramsay, R. R.; Steenkamp, D. J.; Husain, M. *Biochem. J.* **1987**, *241*, 883−892.
(23) Galliani, G.; Monti, D.; Speranza, G.; Manitto, P. *Tetrahedron Lett.* **1984**, *25*, 6037−6040.
(24) Galliani, G.; Monti, D.; Speranza, G.; Manitto, P. *Experientia* **1985**, *41*, 1559−1560.
(25) McDonagh, A. F. In *The Porphyrins*, Vol. VI, Biochemistry Part A.; Dolphin, D., Ed.; Academic Press: New York, 1979; pp 293−491.
(26) Lightner, D. A. In *Bilirubin*, Vol. 1, Chemistry; Heirwegh, K. P. M., Brown, S. B., Eds.; CRC Press: Boca Raton, FL, 1982; pp 1−58.
(27) McDowell, M. T.; Lagarias, J. C. *Plant Physiol.* **2001**, *126*, 1546−1554.
(28) Marko, H.; Muller, N.; Falk, H. *Monatsh. Chem.* **1989**, *120*, 591−595.
(29) Wagner, U. G.; Muller, N.; Schmitzberger, W.; Falk, H.; Kratky, C. *J. Mol. Biol.* **1995**, *247*, 326−337.
(30) Sugishima, M.; Sakamoto, H.; Higashimoto, Y.; Noguchi, M.; Fukuyama, K. *J. Biol. Chem.* **2003**, *278*, 32352−32358.

(Figure 7). This assignment is supported by the absorption spectrum of a BV model compound that is constrained to a porphyrin-like conformation via a bridging linkage between vinyl groups.[31] Both the long wavelength absorption maximum of this model compound and the ratio of its near UV to visible absorption bands, an indicator of bilin conformation, are in good agreement with those of the PcyA:bilin adducts. The small size of the near-infrared absorption maxima of PcyA:BV complexes suggests that the bilin substrate is not fully protonated by the enzyme. In this regard, it has been shown that the pK_a of the linear tetrapyrrole system is considerably lowered if the bilin is constrained to a cyclic conformation.[31] Since free rotation can occur about the terminal methine bridge to produce more extended conformations for "unconstrained" bilins in solution, this not only leads to an increase in the basicity of the tetrapyrrole nitrogen atom but also considerably alters the bilin's absorption spectrum upon protonation.[20,31] Based on these considerations, we propose that the PcyA protein constrains its bilin substrate into a cyclic conformation which enables a proton-donating side chain (D_0) to partially protonate the bilin substrate on a nitrogen atom (see Figure 7).

In the case of the natural BV substrate, exo-vinyl reduction was shown to precede endo-vinyl reduction.[7] We hypothesize that this regiospecificity is achieved by the presence of proton-donating side chains D_1 and D_2 in the enzyme which can more efficiently protonate either C18^2 or O19 atoms as depicted in Figure 7. We envisage that electron transfer to the protonated BV substrate complex yields species **1**, a process that is followed by (or simultaneous with) proton transfer from D_1 to either C18^2 or O19 positions to yield resonance-delocalized radicals **2** and **3**. The O-protonation pathway to produce **3** is interesting, since it could rapidly convert into the C18^2-protonated species **2** via a facile intramolecular rearrangement mechanism shown in Figure 7. While the latter mechanism depends on the vinyl group geometry, an O-protonation pathway provides a plausible explanation for the kinetic preference of exo-vinyl group reduction by PcyA, i.e., intramolecular vs intermolecular proton transfer. We envisage that reduction of the exo-vinyl group is completed upon addition of a second electron to the protonated radical **2** which undergoes a second protonation at C18.[1] We favor this overall mechanism to one involving hydrogen atom abstraction from a residue(s) within the enzyme, based on the stability of the radical intermediate and the results of BV13 reduction described subsequently.

By analogy with the proposed mechanism of exo-vinyl group reduction, we propose a similar pathway for endo-vinyl reduction involving proton-donating residues D_3 and D_4 as shown in Figure 7. In this case, spectroscopic evidence supporting the formation of both one- and two-electron reduced intermediates was obtained using the symmetric substrate BV13. One-electron reduction of the N-protonated BV substrate complex is expected to yield the intermediate **5**, which could be protonated by protein residue D_3 on the C2 or O1 atoms to yield the resonance-delocalized radical species **6** or **7**. While both radical species could then abstract a hydrogen atom from the enzyme, our spectroscopic analyses support a mechanism involving the second electron transfer followed by a rate-limiting protonation of the two-electron-reduced MHBV species **8** and/or **9**. At present, it is not possible to distinguish between C- and O-protonation pathways or whether both can occur in parallel. With regard to the second protonation step, it is interesting that PcyA affords a mixture of 3*Z*- and 3*E*-PCB product. This suggests that the unprotonated MHBV13 intermediate(s) **8** and/or **9** can conformationally equilibrate prior to accepting the second proton from protein residue D_4. By contrast with PcyA, HY2-mediated BV reduction yields primarily the 3*Z*-isomer of PΦB,[27] indicating that its catalytic intermediate(s) is more constrained by the HY2 enzyme. This suggests that modifications in the FDBR catalytic site can "tune" the product isomer mixture. This may have important implications for the stereospecific assembly of phycobiliproteins, which possess bilin-protein linkages with various stereochemistries and regiospecificities.[32]

Considerable experimental work is needed to test these mechanistic hypotheses. In this regard, preliminary site-directed mutagenesis and chemical modification studies implicate two conserved histidine residues specific to the PcyA family of enzymes in the reduction of the exo-vinyl group (Tu, S.-L.; Lagarias, J. C. Unpublished data). For this reason, we have indicated proton-donating residues D_1 and D_2 to be cationic in our proposed mechanism. During catalysis, positively charged imidazolium side chains would become neutral contributing to a more hydrophobic environment for the bilin substrate, a process that may enhance the binding of the DHBV intermediate, preventing its release from the enzyme. We envisage proton-donating residues D_0, D_3, and D_4 to contain carboxyl groups which might promote product release upon their ionization during catalysis. Site-directed mutagenesis of conserved aspartic acid and glutamic acid residues that might perform these functions is in progress. These experiments, along with pulsed EPR and stopped-flow measurements using isotopically labeled substrates and substrate analogues, should provide a detailed picture of the catalytic mechanism of this biologically important family of radical enzymes.

Experimental Procedures

Materials. All the chemicals are ACS grade unless otherwise specified. NADPH (Cat. No.N-1630), ferredoxin:NADP$^+$ oxidoreductase (FNR) (Cat. No.F-0628), glucose oxidase (Cat. No.G6125), catalase (Cat No.C-40), and glutathione agarose (Cat. No.G4510) were purchased from Sigma. Bovine serum albumin (Cat. No.100-018) was purchased from Boehringer-Mannheim. Superdex 200 gel filtration matrix, expression vector pGEX-6P-1, and PreScission protease were purchased from Amersham Pharmacia Biotech. HPLC grade acetone, acetonitrile, formic acid, and spectroanalytical grade glycerol were obtained from Fisher. The Ultrafree-4 concentrator was purchased from Millipore Corporation. Sep-Pak Light cartridges were obtained from Waters (Cat. No.WAT023501). The BCA protein assay reagents were purchased from Pierce (Cat. No. 23228). Biliverdin IXα was prepared as described previously.[33,34] Biliverdin XIIIα was kindly provided by Dr. Tony McDonagh (UCSF).

Recombinant PcyA and Ferredoxin Preparations. Expression and purification of recombinant *Anabaena* sp. PCC 7120 PcyA were performed as described previously.[7] PcyA protein was further purified with a Superdex 200 size exclusion column pre-equilibrated with 20

(31) Krois, D. *Monatsh. Chem.* **1991**, *122*, 495−506.

(32) Schluchter, W. M.; Glazer, A. N. In *The Photosynthetic Prokaryotes*; Peschek, G. A., Loffelhardt, W., Schmetterer, G., Eds.; Kluwer Academic/Plenum Press: New York, 1999; pp 83−95.

(33) Cornejo, J.; Beale, S. I.; Terry, M. J.; Lagarias, J. C. *J. Biol. Chem.* **1992**, *267*, 14790−14798.

(34) Elich, T. D.; McDonagh, A. F.; Palma, L. A.; Lagarias, J. C. *J. Biol. Chem.* **1989**, *264*, 183−189.

mM Tris-HCl pH 8.5 buffer containing 100 mM NaCl, followed by dialysis against TKK buffer (25 mM TES−KOH pH 8.5 containing 100 mM KCl) and 10% (v/v) glycerol. Recombinant *Synechococcus* sp. PCC7002 ferredoxin was expressed and purified as described previously.[35] Purified ferredoxin was dialyzed against TKK buffer. Both PcyA and ferredoxin preparations (>10 mg/mL concentration) were stored frozen at −80°C prior to use.

Anaerobic Bilin Reductase Assay and HPLC Analyses. Anaerobic bilin reductase assays were performed under green safe light essentially as described previously[1,27] with the following modifications. All buffers were vacuum-degassed prior to preparation. Reaction mixtures for standard assays were prepared in TKK buffer containing 10 μM PcyA, 10 μM BV, 0.0025 U/ml FNR (3 nM final concentration), 10 μM ferredoxin, 10 μM bovine serum albumin, and an oxygen scavenging system (50 U/ml glucose oxidase, 100 mM glucose and 50 U/ml catalase). Reaction mixtures were incubated with stirring at 16 °C in septum-stoppered quartz cuvettes over which 99% pure N_2 was passed for 30 min. To initiate catalysis, measured aliquots of NADPH from stock solutions made anaerobic by the addition of the oxygen scavenging system were injected into reaction mixtures in cuvettes using a gastight syringe. NADPH stock solutions were quantified using $\epsilon_{340} = 6220\ M^{-1}\ cm^{-1}$. Absorbance spectra were recorded using an HP 8453 diode array spectrophotometer to monitor the course of catalysis. A thermostatable cell holder and cell stirring module were used to control the reaction temperature and to mix the reaction mixture. For HPLC analysis (below), 200 μL aliquots of reaction mixtures were withdrawn with a gastight syringe, and crude bilins were extracted/eluted using C18 Sep-Pak Light cartridges followed by evaporation to dryness using a SpeedVac concentrator.[7] Crude bilins were dissolved in 10 μL of DMSO, diluted with 190 μL of HPLC mobile phase, and filtered with 0.45 μm poly(tetrafluoroethylene) syringe filters prior to injection onto a 4.6 × 250 mm^2 Phenomenex Ultracarb 5 μm ODS (20) reverse-phase column equipped with a 4.6 × 30 mm^2 guard column of the same material. The mobile phase consisted of 50% acetone and 50% 20 mM formic acid (by volume), and the flow rate of 0.6 mL/min was adjusted using an Agilent Technologies 1100 liquid chromatograph.[7] The eluate was monitored with an Agilent Technologies 1100 diode array detector. Authentic bilin standards for BV, BV13, 18^1,18^2-DHBV, 3*Z*- and 3*E*-PCB, and 3*Z*- and 3*E*-isoPΦB were obtained as described previously.[7]

Global Spectral Analysis. The global kinetic spectral fitting program SpecFit32 (Spectrum Software Associates) was used to determine spectra of the PcyA:BV13 substrate, the semireduced intermediate, and the PcyA:isoPΦB product complexes formed during the course of BV13 reduction. For global spectral determination, the experiment was performed under standard anaerobic assay conditions as described above. The reaction was initiated by the addition of 5 μM NADPH (i.e., one electron equiv). The kinetic spectral data for this reaction were initially fitted to a full set of chemical equations that include the NADPH-dependent FNR generation of reduced ferredoxin (Fd_{red}), the one-electron transfer from Fd_{red} to the PcyA:BV13 substrate complex, the one-electron transfer from Fd_{red} to the PcyA:MHBV13$^\bullet$ radical intermediate complex, and the disproportionation of two PcyA^{1-}:MHBV13$^\bullet$ radical intermediates. The fit to this complete mechanism was reasonable but not wholly satisfactory; the lack of knowledge of the rate constants for the reactions involving FNR made the analysis difficult. Therefore, a simpler kinetic model was used (eqs 1 and 2).

$$Fd_{red} + PcyA{:}BV13 \rightarrow Fd_{ox} + PcyA^{1-}{:}MHBV13^{\bullet} \quad (1)$$

$$PcyA^{1-}{:}MHBV13^{\bullet} + PcyA^{1-}{:}MHBV13^{\bullet} \rightarrow PcyA{:}BV13 + PcyA^{2-}{:}isoP\Phi B \quad (2)$$

These equations describe the one-electron reduction of the PcyA:BV13 complex by reduced ferredoxin (eq 1), followed by the disproportionation of two one-electron reduced complexes to reactant and final product (eq 2). The only colored species defined in SpecFit were PcyA:BV13, PcyA^{1-}:MHBV13$^\bullet$, and PcyA^{2-}:isoPΦB. This model was found to fit well the kinetic data in the spectral range from 300 to 900 nm. The main assumption associated with using this simpler model is that Fd_{red} is present at a constant concentration. This is expected to be true, since reduced ferredoxin is produced by FNR in what is probably the rate-limiting step for reduction of PcyA:BV13 (i.e., FNR concentration is only 3 nM), and Fd_{red} is rapidly consumed in the reaction described by eq 1. Preliminary stopped-flow measurements of PcyA:BV13 reduction by prereduced ferredoxin show the reaction to be very fast (Tu, S.-L.; Toney, M. D.; and Lagarias, J. C. Unpublished data). Thus, Fd_{red} rapidly builds up to a low, constant steady-state concentration, and the reaction in eq 1 is pseudo-first-order in PcyA:BV13. In view of their modest absorption coefficients in this spectral range or their low concentration, the contributions of Fd_{red}, Fd_{ox}, and FNR were expected to be neglible compared with those of the bilin−protein complex, and for this reason, they were ignored in the global spectral analyses. To further validate the spectra obtained from the global analysis of the kinetic data, spectra of independently prepared PcyA:BV13 substrate and PcyA:isoPΦB product complexes were recorded. Both spectra were in excellent agreement with those deduced by the SpecFit analysis.

Absorption Spectra Curve-Fitting and Semiempirical Absorption Spectra Calculations. The global analysis-derived absorption spectra of the PcyA:BV13 substrate, the PcyA^{1-}:MHBV13$^\bullet$ intermediate, and the PcyA:isoPΦB product complexes were fitted with log-normal curves using the PeakFit program (Systat Software) to resolve individual transitions.[36] Correlation coefficients of 0.999 were obtained for all simulated spectra when compared with the experimental absorption spectra obtained from global fitting. Absorption spectra were calculated for various tautomers and protonated forms of BV13 substrate, isoPΦB product, and three potential intermediate species: the semireduced/unprotonated BV13$^{\bullet-}$ radical anion, the semireduced/protonated MHBV13H$^\bullet$ neutral radical, and the fully reduced/unprotonated MHBV13H$^-$ anion. To optimize the molecular geometries of these species, AM1 calculations[37] were first performed using the Gaussian 98W suite of programs.[38] For these calculations, bilins were initially constructed in porphyrin-like "cyclic" configurations and the two propionate side chains were substituted with methyl groups. These cyclic configurations were maintained in the optimizations without employing constraints. ZINDO calculations were also performed using Gaussian 98W to obtain the electronic transitions (i.e., absorption spectra) of each AM1 optimized structure.[39]

Freeze-Quench EPR Measurements. For EPR measurements, the anaerobic assay described above was used with the exception that concentrations of PcyA, BV, and FNR were all increased 4-fold (to 40 μM, 40 μM, and 12 nM, respectively) and 15% spectro-analytical grade

(35) Schluchter, W. M. Ph.D. Dissertation, Pennsylvania State University: University Park, PA, 1994.
(36) Siano, D. B.; Metzler, D. E. *J. Chem. Phys.* **1969**, *51*, 1856−1861.
(37) Dewar, M. J. S.; Zoebisch, E. G.; Healy, E. F. *J. Am. Chem. Soc.* **1985**, *107*, 3902−3909.
(38) Frisch, M. J.; Trucks, G. W.; Schlegel, H. B.; Scuseria, G. E.; Robb, M. A.; Cheeseman, J. R.; Zakrzewski, V. G.; Montgomery, J. J. A.; Stratmann, R. E.; Burant, J. C.; Dapprich, S.; Millam, J. M.; Daniels, A. D.; Kudin, K. N.; Strain, M. C.; Farkas, O.; Tomasi, J.; Barone, V.; Cossi, M.; Cammi, R.; Mennucci, B.; Pomelli, C.; Adamo, C.; Clifford, S.; Ochterski, J.; Petersson, G. A.; Ayala, P. Y.; Cui, Q.; Morokuma, K.; Malick, D. K.; Rabuck, A. D.; Raghavachari, K.; Foresman, J. B.; Cioslowski, J.; Ortiz, J. V.; Baboul, A. G.; Stefanov, B. B.; Liu, G.; Liashenko, A.; Piskorz, P.; Komaromi, I.; Gomperts, R.; Martin, R. L.; Fox, D. J.; Keith, T.; Al-Laham, M. A.; Peng, C. Y.; Nanayakkara, A.; Gonzalez, C.; Challacombe, M.; Gill, P. M. W.; Johnson, B. G.; Chen, W.; Wong, M. W.; Andres, J. L.; Head-Gordon, M.; Replogle, E. S.; Pople, J. A. Gaussian, Inc.: Pittsburgh, PA, 1998.
(39) Zerner, M. C. In *Reviews of Computational Chemistry*; Lipkowitz, K. B., Boyd, D. B., Eds.; VCH Publishing: New York, 1991; Vol. 2.

glycerol was included in the reaction mixtures. At various times after addition of NADPH, absorption spectra were recorded and 200 μL aliquots were withdrawn from reaction mixtures, transferred to 4 mm quartz EPR tubes, and immediately frozen in liquid nitrogen. Continuous wave EPR studies of PcyA were performed using a Bruker ECS106 spectrometer. EPR spectra at 15 K were acquired using the X-band microwave frequency of 9.69 GHz with a modulation amplitude of 4 G. The temperature of the sample was maintained using an Oxford ESR900 liquid helium cryostat and an Oxford ITC 503 temperature controller.

Acknowledgment. This work was supported in part by grants from USDA CRGI AMD-0103397 (to J.C.L.), NIH GM48242 (to R.D.B.), and NIH GM54779 (to M.D.T.).

Supporting Information Available: Structures used for the AM1 and ZINDO calculations shown in Table 1 (PDF). This material is available free of charge via the Internet at http://pubs.acs.org.

JA049280Z